Carbohydrate Research 361 (2012) 182–188

Contents lists available at SciVerse ScienceDirect

Carbohydrate Research

journal homepage: www.elsevier.com/locate/carres

# Conformational behavior of peracetylated β-D-mannopyranosyl methanesulfonamide: implications for the mechanism of sulfonamidoglycosylation of carbohydrate derivatives

Martín J. Lavecchia [b], Oscar M. Rodríguez [a], Gustavo A. Echeverría [c], Reinaldo Pis Diez [b,*], Pedro A. Colinas [a,*]

[a] LADECOR, Departamento de Química, Facultad de Ciencias Exactas, Universidad Nacional de La Plata, 47 y 115, 1900 La Plata, Argentina
[b] CEQUINOR, Centro de Química Inorgánica (CONICET, UNLP), Departamento de Química, Facultad de Ciencias Exactas, Universidad Nacional de La Plata, CC 962, 1900 La Plata, Argentina
[c] LANADI e IFLP (CCT-La Plata), Departamento de Física, Facultad de Ciencias Exactas, Universidad Nacional de La Plata, CC 67, 1900 La Plata, Argentina

ARTICLE INFO

*Article history:*
Received 1 July 2012
Received in revised form 14 August 2012
Accepted 28 August 2012
Available online 6 September 2012

*Keywords:*
Glycosyl sulfonamides
Sulfonamidoglycosylation
*endo*-Anomeric effect
*exo*-Anomeric effect
Density functional theory

ABSTRACT

The conformational behavior of 2,3,4,6-tetra-*O*-acetyl-β-D-mannopyranosyl methanesulfonamide has been investigated from a combined theoretical and experimental point of view. The study of the conformational space of the glycosyl sulfonamide revealed that the β anomer is thermodynamically more stable than the α one. This fact suggests that the synthesis reaction could take place mainly under thermodynamic control as the main experimental product is the β-anomeric form of the sulfonamide. Several intramolecular hydrogen bonds were found in the stable conformers of the *N*-mannopyranosyl sulfonamide under study. A relationship was found to exist between them and the relative stability of the conformers. A detailed analysis of geometrical parameters shed light into the nature of the solid state structure of the novel 2,3,4,6-tetra-*O*-acetyl-β-D-mannopyranosyl methanesulfonamide in terms of *exo*- and *endo*-anomeric effects and antiperiplanar relationships. NBO calculations confirmed those findings. Calculated $^{1}H$ and $^{13}C$ NMR chemical shifts support previous findings concerning configuration and conformation assignments of the title sulfonamide.

Finally, an explanation of the stereochemical outcome of sulfonamidoglycosylations, was given in terms of *exo*- and *endo*-anomeric effects and steric factors.

© 2012 Elsevier Ltd. All rights reserved.

## 1. Introduction

In many cases, use of carbohydrates as drugs has an important drawback: they are sensitive to the presence of enzymes and acidic or basic media. Thus, design of mimetics that bind to enzymes but are not processed to product in the usual way is an active area of research.[1] In recent years a variety of replacements for the glycosidic linkage have raised considerable interest as stable carbohydrate mimetics due to their enormous stability to enzymatic degradation and the resulting possibilities as enzyme inhibitors.[2] The most common modifications with respect to the linkage are S-glycosides, C-glycosides, and N-glycosides. An unusual enzyme-resistant replacement for the glycosidic linkage, is the sulfonamide corresponding to a glycosylamine carrying a sulfonyl group at nitrogen. However, glycosylamines are not stable and are very sensitive to hydrolysis and anomerization.[3] To overcome this problem, one of our groups has developed several syntheses of *N*-glycosyl sulfonamides by sulfonamidoglycosylation of carbohydrate derivatives.[4] These sulfonamidoglycosides have been shown to possess interesting biological activities. In that sense, recently we reported the synthesis of a series of α-D-hex-2-enopyranosyl sulfonamides, which were evaluated against human hepatocellular liver carcinoma (HepG2) and human lung adenocarcinoma (A549) cell lines and showed antiproliferative activity in the micromolar range.[5] Very recently we have prepared novel *N*-β-glycosyl sulfonamides and shown that they selectively target cancer-associated CAs (IX and XII) with $K_I$s in the low nanomolar range.[6]

The stereochemical outcome of sulfonamidoglycosylations is quite different depending on the reactives and products.[4] To shed some light on the mechanism of these reactions, we have studied the conformational behavior of peracetylated *N*-D-mannopyranosyl methanesulfonamide in solution, in the solid state and from a theoretical point of view.

## 2. Results and discussion

As anomers of 2,3,4,6-tetra-*O*-acetyl-D-mannopyranosyl methanesulfonamide could be present in two equilibrium

* Corresponding authors.
*E-mail addresses:* pis_diez@quimica.unlp.edu.ar (R. Pis Diez), pcolinas@quimica.unlp.edu.ar (P.A. Colinas).

0008-6215/$ - see front matter © 2012 Elsevier Ltd. All rights reserved.
http://dx.doi.org/10.1016/j.carres.2012.08.016

conformations, namely $^1C_4$ and $^4C_1$, two different starting conformations of the glycosyl sulfonamide are considered for each anomer. These conformations are labeled **1**–**4**, see Figure 1.

The crystal structure of 2,3,4,6-tetra-*O*-acetyl-β-D-mannopyranosyl methanesulfonamide is shown in Figure 2. It can be seen that this anomer adopts a $^4C_1$ conformation and the acetoxymethyl group at C5 in an equatorial position in the crystal lattice.

The study of the conformational space of 2,3,4,6-tetra-*O*-acetyl-D-mannopyranosyl methanesulfonamide leads to six different conformations both in the gas phase and after solvent effects are included. Three of those conformations belong to the β anomeric form, whereas the remaining ones represent the α anomer. Table 1 lists some selected geometrical parameters for the stable conformations. Gibbs free energies, also shown in Table 1, are slightly affected by the inclusion of solvent effects. Conformer **3c** becomes less stable by more than 1 kcal mol$^{-1}$ relative to the more stable conformer when solvent effects are accounted for, whereas conformers **2a** and **1a** invert their relative order. Gibbs free energies calculated in the gas phase indicate that the relative composition at 298.15 K is about 97% of the β anomer of peracetylated *N*-D-mannopyranosyl methanesulfonamide and about 3% of the α form. When solvent effects are taken into account, the relative composition is almost unaffected with about 98% for the β anomer and the remaining 2% for the α anomer, a result which is in excellent agreement with experimental reports.[7] It is very interesting to note that the inclusion of solvent effects has little impact on the gas phase geometries, see Table 1. Conformational behavior about the C5–C6 bond in carbohydrates leads to three staggered orientations namely *gauche-gauche* (*gg*), *trans-gauche* (*tg*), and *gauche-trans* (*gt*). All these conformations correspond to local minima on the molecular surface of the corresponding carbohydrate. Conformers **3a**, **3b**, **1a**, and the solid state structure, show preference for conformation *gt* while *gg* is preferred for conformer **3c**, and *tg* is preferred for conformers **2a** and **2b**. It should also be noted that four stable conformers (**3a**–**c**, **1a**) reported in this work exhibited the $^4C_1$ conformation with $\tau$(C1–O5–C5–C4), $\tau$(O5–C1–C2–C3), and $\tau$(C2–C3–C4–C5–O5) dihedral angles around the ideal value of +60°; $\tau$(C1–C2–C3–C4), $\tau$(C5–O5–C1–C2) around −60° and the acetoxymethyl group at C5 in a equatorial position. On the other hand the conformers **2a** and **2b** showed a $^1C_4$ conformation with the acetoxymethyl group at C5 in an axial position. It can also be seen from the table that other torsion angles such as $\tau$(N1–C1–C2–C3), $\tau$(N1–C1–O5–C5), $\tau$(C2–C1–N1–S1), and $\tau$(O5–C1–N1–S1) indicate that the solid structure adopts the β anomeric form. It is also of interest to compare some selected bond lengths and bond angles involving the O5–C1–N1 acetal moiety in the different conformers with experimental data. The calculated O5–C1–N1 bond angle in the three equatorially substituted conformers **3**

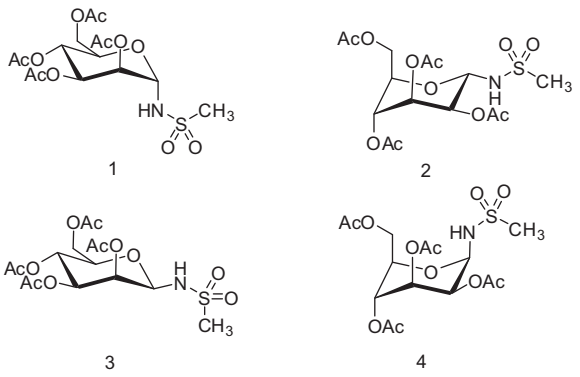



**Figure 1.** Schematic representation of the four starting conformations of 2,3,4,6-tetra-*O*-acetyl-D-mannopyranosyl methanesulfonamide. 1 and 2 correspond to the α anomeric form and 3 and 4 represent the β one.

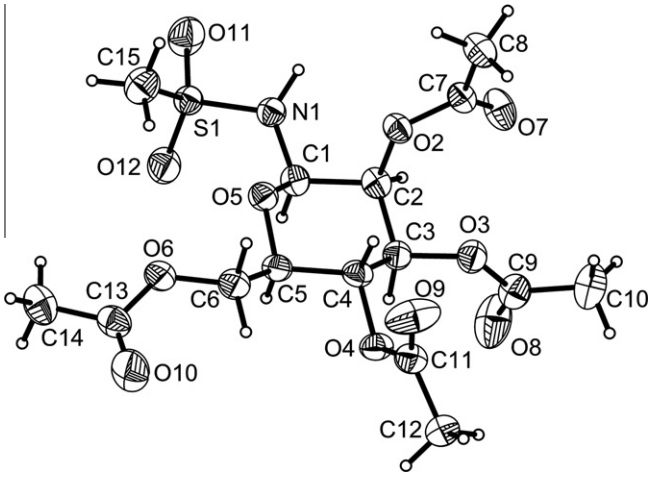



**Figure 2.** Drawing of 2,3,4,6-tetra-*O*-acetyl-β-D-mannopyranosyl methanesulfonamide showing the labeling of the non-H atoms and their displacement ellipsoids at the 30% probability level.

agrees very well with the crystal structure results (**3a**: 109.8° (110°); **3b**: 109.6° (109.6°), and **3c**: 109.6° (109.6°); experimental: 109.3°, calculated values in acetonitrile are in parenthesis). On the other hand, the O5–C1–N1 bond angle calculated for the axially substituted conformer **1a** (111.2° (111.0°)) is considerably higher than the experimental value. These facts are in good agreement with previous studies of bond angle variations in acetals.[8] It is important to point out that conformers **2a** and **2b** exhibited the $^1C_4$ conformation and the substituent at the anomeric center adopts an equatorial position so the O5–C1–N1 bond angle resembles the values found in the β-anomers. The C1–N1 bond length in conformers **3** (**3a**: 1.430 Å (1.440 Å); **3b**: 1.431 Å (1.439 Å); **3c**: 1.431 Å (1.441 Å)), in the solid-state conformation of the β anomer (1.431 Å) and conformers of α-anomer with a $^1C_4$ conformation (**2a**: 1.428 Å (1.435 Å); **2b** 1.428 (1.436 Å)) are shorter than the value in conformer **1a** (1.464 Å (1.469 Å)). These findings could be explained in terms of a competition between a $n_{N1} \rightarrow \sigma^*_{C1-O5}$ orbital interaction (*exo*-anomeric effect) and a $n_{O1} \rightarrow \sigma^*_{C1-N1}$ interaction (*endo*-anomeric effect) in $^4C_1$ conformer of α anomer (**1a**). In the conformers **3** of the β anomer, and the $^1C_4$ conformers of α anomer (**2**a and **2b**) the *endo*-anomeric effect is not present, and then, a dominant $n_{N1} \rightarrow \sigma^*_{C1-O5}$ leads to a shorter C1-N1 bond. As can be seen in Table 1 the values of the torsion angle $\tau$(C2–C1–N1–S1) show an antiperiplanar relationship in conformers **3**, **2a**, **2b**, and in the solid state, in agreement with the $n_{N1} \rightarrow \sigma^*_{C1-O5}$ orbital interaction associated with the exo-anomeric effect. The NBO analysis presented in Table 2 shows that the $n_{N1} \rightarrow \sigma^*_{C1-O5}$ is similar for both anomers except for conformer **1a**, whereas $n_{O5} \rightarrow \sigma^*_{C1-N1}$ orbital interaction is higher in this conformer, thus supporting the experimental findings.

The conformational preference of the β anomer in solution is similar to that in the solid state since spin-spin coupling constant data indicate a value of 10.5 Hz for $J_{N1H-C1H}$,[7] which is consistent with the presence of an antiperiplanar relationship between N1H and H atom bound to C1. Thus, conformations predicted about the glycosyl linkage in conformers **3** are in very good agreement with the experimental data both in solution and in solid state.

Table 3 shows some characteristic geometric parameters and topological properties of intramolecular hydrogen bonds found for the stable conformers of the title compound. The values of the density and the Laplacian of the density at the bond critical points indicate that these are effectively hydrogen bonds. The evaluation of the stabilization energy as a consequence of the formation of an intramolecular hydrogen bond is a controversial

**Table 1**
Selected torsion angles ($\tau$, in degrees), bond angle ($\alpha$, in degrees), and bond lengths ($r$, in Å) of the six stable conformers of 2,3,4,6-tetra-*O*-acetyl-D-mannopyranosyl methanesulfonamide found within 3 kcal mol$^{-1}$ with respect to the most stable one in the gas phase

| | **3a** | **3b** | **3c** | **2a** | **1a** | **2b** | **Exp.** |
|---|---|---|---|---|---|---|---|
| $\tau$(C1–O5–C5–C4) | 62.43 | 61.99 | 62.13 | −53.02 | 57.01 | −54.59 | 66.03 |
| | (62.3) | (61.91) | (61.35) | (−53.02) | (57.87) | (−53.49) | |
| $\tau$(C4–C5–C6–O3) | −170.89 | −171.20 | 58.48 | −59.57 | −164.18 | −80.16 | 178.82 |
| | (−172.71) | (−173.77) | (58.12) | (−56.07) | (−173.35) | (−80.97) | |
| $\tau$(O5–C5–C6–O3) | 68.79 | 68.33 | −63.40 | 172.90 | 74.60 | 152.12 | 60.49 |
| | (67.67) | (66.57) | (−63.39) | (176.99) | (67.22) | (151.5) | |
| $\tau$(N1–C1–C2–C3) | 175.69 | 175.73 | 175.01 | 179.33 | −70.60 | 178.85 | 177.42 |
| | (179.05) | (179.01) | (178.87) | (−176.43) | (−73.85) | (−177.3) | |
| $\tau$(N1–C1–O5–C5) | 175.98 | 176.01 | 177.19 | −177.62 | 66.12 | −176.19 | 171.75 |
| | (172.07) | (172.46) | (174.49) | (179.78) | (67.24) | (−179.33) | |
| $\tau$(C2–C1–N1–S1) | 162.31 | 163.50 | 163.42 | −164.43 | −149.18 | −166.65 | 170.39 |
| | (159.04) | (159.04) | (163.9) | (−157.45) | (−158.08) | (−159.6) | |
| $\tau$(O5–C1–N1–S1) | −75.84 | −74.81 | −74.31 | 77.02 | 87.39 | 75.35 | −67.69 |
| | (−78.07) | (−77.7) | (−72.96) | (82.86) | (78.25) | (81.36) | |
| $\tau$(O5–C1–C2–C3) | 54.28 | 54.41 | 53.29 | −60.82 | 52.91 | −61.53 | 56.02 |
| | (56.65) | (56.32) | (56.23) | (−56.78) | (49.29) | (−58.03) | |
| $\tau$(C1–C2–C3–C4) | −51.98 | −51.53 | −51.98 | 54.54 | −53.26 | 54.60 | −52.43 |
| | (−52.85) | (−53.27) | (−54.13) | (51.92) | (−50.98) | (52.84) | |
| $\tau$(C5–O5–C1–C2) | −62.03 | −62.22 | −60.73 | 61.71 | −56.66 | 63.33 | −65.73 |
| | (−64.13) | (−63.37) | (−62.2) | (59.29) | (−54.72) | (60.42) | |
| $\tau$(C2–C3–C4–C5) | 52.99 | 51.88 | 53.71 | −45.43 | 53.44 | −45.40 | 55.34 |
| | (52.89) | (53.62) | (54.85) | (−45.84) | (54.53) | (−46.1) | |
| $\tau$(C3–C4–C5–O5) | −56.08 | −54.91 | −56.83 | 43.07 | −53.50 | 43.65 | −59.48 |
| | (−55.23) | (−55.55) | (−56.29) | (44.48) | (−55.87) | (44.36) | |
| $\alpha$(O5–C1–N1) | 109.60 | 109.64 | 109.77 | 109.63 | 111.21 | 109.68 | 109.32 |
| | (109.57) | (109.59) | (109.97) | (108.97) | (111.01) | (108.88) | |
| r(O5–C1) | 1.4360 | 1.4348 | 1.4373 | 1.4448 | 1.4188 | 1.4459 | 1.4348 |
| | (1.4327) | (1.4325) | (1.4326) | (1.4406) | (1.4180) | (1.4394) | |
| r(C1–N1) | 1.4307 | 1.4315 | 1.4295 | 1.4285 | 1.4642 | 1.4283 | 1.4308 |
| | (1.4393) | (1.4409) | (1.4401) | (1.4355) | (1.4695) | (1.4352) | |
| $\Delta G$ (kcal/mol) | 0.00 | 0.63 | 0.93 | 2.19 | 2.73 | 2.98 | |
| | (0.00) | (0.47) | (2.15) | (3.50) | (2.17) | (4.86) | |
| % | 62.74 | 21.68 | 13.03 | 1.53 | 0.61 | 0.40 | |
| | (66.41) | (29.97) | (1.74) | (0.18) | (1.69) | (0.02) | |
| RMSD | 0.33 | 0.36 | 1.15 | – | – | – | |
| | (0.41) | (0.33) | (1.20) | – | – | – | |

Results obtained when solvent effects are included are shown in parenthesis. Comparison with experimental data is also provided. Gibbs free energies, in kcal mol$^{-1}$, relative to the most stable conformer and percent contribution of every conformation are also shown. The root-mean-square deviation of conformers **3** with respect to solid state structure is also listed.

**Table 2**
Natural bond orbital interaction energies, in kcal mol$^{-1}$, of the different conformers calculated for 2,3,4,6-tetra-*O*-acetyl-D-mannopyranosyl methanesulfonamide in the gas phase

| | **3a** | **3b** | **3c** | **1a** | **2a** | **2b** | **Exp.** |
|---|---|---|---|---|---|---|---|
| $n_{O5} \rightarrow \sigma^*_{C1-N1}$ | 2.42 | 2.44 | 2.41 | 11.42 | 2.53 | 2.61 | 2.33 |
| | (2.29) | (2.36) | (2.28) | (11.47) | (2.77) | (2.76) | |
| $n_{N1} \rightarrow \sigma^*_{C1-O5}$ | 15.16 | 15.56 | 15.25 | 8.45 | 16.79 | 16.61 | 15.46 |
| | (14.95) | (14.38) | (15.02) | (6.24) | (14.29) | (14.22) | |

Results obtained when solvent effects are included are shown in parenthesis. The column labeled Exp. shows the NBO analysis carried out on the frozen solid state geometry at the B3LYP/6-31++G(d,p) level of theory.

subject. Considering that the change in the equilibrium geometries is almost negligible when solvent effects are accounted for, the difference in Gibbs free energies with and without solvent effects is taken as a candidate to rationalize the stabilization energy due to the presence of intramolecular hydrogen bonds. Moreover, those values are related to the difference in the values of the electronic density at the bond critical points for the intramolecular hydrogen bonds found in every conformer. Gibbs free energy difference ($\Delta G_{\text{solvent}-\text{gas}}$) and difference in the electronic density at the bond critical points ($\Delta P_{\text{solvent}-\text{gas}}$) are defined as

$$\Delta G_{\text{solvent}-\text{gas}} = G_{\text{solvent}} - G_{\text{gas}}$$

$$\Delta P_{\text{solvent}-\text{gas}} = \sum_i \rho i, \text{solvent} - \sum_i \rho i, \text{gas}$$

where $G$ is the Gibbs free energy obtained after adding thermal corrections to the total electronic energy and the sums run over all the intramolecular hydrogen bonds of every conformer both in the gas phase and when solvent effects are included. Negative values of $\Delta G_{\text{solvent}-\text{gas}}$ indicate that the inclusion of solvent effects leads to a further stabilization with respect to conformations in the gas phase. Positive values of $\Delta P_{\text{solvent}-\text{gas}}$, on the other hand, show that a reinforcement in the strength of hydrogen bonds takes place after solvent effects are accounted for. According to Table S1 (See Supplementary Data), the relative ordering of conformers in terms of increasing $\Delta G_{\text{solvent}-\text{gas}}$ is **1a > 3b > 3a > 3c > 2a > 2b**. Interestingly, the same relative ordering is obtained for decreasing $\Delta P_{\text{solvent}-\text{gas}}$. It can be seen in Figure 3 that a good linear relationship exists between $\Delta G_{\text{solvent}-\text{gas}}$ and $\Delta P_{\text{solvent}-\text{gas}}$. That relationship suggests that the increase in the strength of the intramolecular hydrogen bonds after the inclusion of solvent effects plays a significant role in the

**Table 3**
Bond lengths ($r$, in Å), bond angles ($\alpha$, in degrees), electron density ($\rho$), Laplacian of the electron density ($\nabla^2\rho$), and bond ellipticity ($\varepsilon$), all in atomic units, of intramolecular hydrogen bonds of the six stable conformers of 2,3,4,6-tetra-*O*-acetyl-D-mannopyranosyl methanesulfonamide found in the present work

| Conformer | Bond | $r$(X···H) | $r$(X···Y) | $\alpha$(X···HY) | $\rho$ | $\nabla^2\rho$ | $\varepsilon$ |
|---|---|---|---|---|---|---|---|
| **3a** | O7···H-C10 | 2.951 | 3.633 | 120.6 | 0.0036 | 0.0143 | 1.2800 |
| | O5···H-C15 | 2.573 | 3.209 | 116.4 | 0.0089 | 0.0327 | 0.2069 |
| | O2···H-C15 | 3.040 | 4.111 | 167.8 | 0.0026 | 0.0116 | 5.3340 |
| | O5···H-C15 | 2.589 | 3.224 | 116.4 | 0.0087 | 0.0319 | 0.2244 |
| | O2···H-C15 | 2.961 | 4.022 | 164.5 | 0.0031 | 0.0131 | 0.5859 |
| **3b** | O7···H-C17 | 2.947 | 3.629 | 120.6 | 0.0036 | 0.0145 | 1.3943 |
| | O5···H-C15 | 2.561 | 3.209 | 117.2 | 0.0090 | 0.0331 | 0.1898 |
| | O2···H-C15 | 2.981 | 4.043 | 164.7 | 0.0030 | 0.0127 | 0.7281 |
| | O5···H-C15 | 2.570 | 3.219 | 117.3 | 0.0090 | 0.0327 | 0.2010 |
| **3c** | O7···H-C10 | 2.994 | 3.630 | 120.9 | 0.0036 | 0.0145 | 1.1372 |
| | O10···H-C15 | 2.799 | 3.619 | 131.9 | 0.0044 | 0.0174 | 0.1342 |
| | O5···H-C15 | 2.581 | 3.254 | 119.1 | 0.0084 | 0.0312 | 0.1930 |
| | O10···H-C15 | 3.027 | 3.849 | 132.6 | 0.0028 | 0.0113 | 0.1353 |
| | O5···H-C15 | 2.576 | 3.252 | 119.3 | 0.0086 | 0.0315 | 0.1901 |
| **2a** | O5···H-C15 | 2.652 | 3.305 | 117.9 | 0.0074 | 0.0278 | 0.2499 |
| | O3···H-C6 | 2.518 | 3.173 | 117.6 | 0.0096 | 0.0355 | 0.2054 |
| | O9···H-C14 | 3.101 | 3.900 | 130.3 | 0.0023 | 0.0095 | 0.3470 |
| | O7···H-N1 | 2.499 | 3.077 | 115.5 | 0.0095 | 0.0360 | 0.5204 |
| | O3···H-C6 | 2.496 | 3.125 | 115.6 | 0.0101 | 0.0376 | 0.2437 |
| | O9···H-C14 | 3.389 | 4.136 | 126.5 | 0.0014 | 0.0056 | 2.1800 |
| | O5···H-C15 | 2.777 | 3.380 | 114.7 | 0.0060 | 0.0232 | 0.6760 |
| **1a** | O5···H-C15 | 2.817 | 3.502 | 120.7 | 0.0054 | 0.0210 | 0.6643 |
| | O2···H-C15 | 3.096 | 3.994 | 140.0 | 0.0025 | 0.0105 | 0.0905 |
| | O5···H-C15 | 2.720 | 3.395 | 119.7 | 0.0067 | 0.0251 | 0.3314 |
| | O2···H-C15 | 2.749 | 3.710 | 146.8 | 0.0053 | 0.0199 | 0.0182 |
| **2b** | O3···H-C6 | 2.495 | 3.200 | 121.3 | 0.0100 | 0.0362 | 0.1531 |
| | O9···H-C14 | 3.373 | 4.150 | 128.9 | 0.0013 | 0.0056 | 1.2841 |
| | O7···H-N1 | 2.399 | 3.033 | 119.6 | 0.0112 | 0.0412 | 0.2789 |
| | O10···H-C4 | 2.708 | 3.498 | 128.9 | 0.0064 | 0.0237 | 0.0970 |
| | O10···H-C10 | 2.586 | 3.444 | 134.6 | 0.0066 | 0.0257 | 0.0997 |
| | O5···H-C15 | 2.654 | 3.314 | 118.4 | 0.0074 | 0.0277 | 0.2408 |
| | O3···H-C6 | 2.466 | 3.127 | 121.4 | 0.0106 | 0.0381 | 0.1481 |
| | O10···H-C4 | 2.701 | 3.489 | 128.7 | 0.0065 | 0.0236 | 0.0539 |
| | O10···H-C10 | 2.666 | 3.803 | 154.5 | 0.0059 | 0.0226 | 0.1476 |
| | O5···H-C15 | 2.728 | 3.337 | 114.9 | 0.0066 | 0.0252 | 0.4393 |

The upper set of data for every conformer corresponds to gas-phase results, whereas the lower set corresponds to C-PCM results.

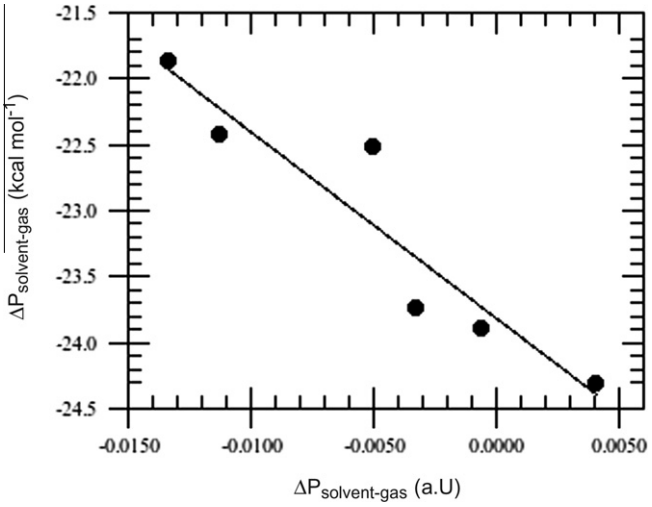



**Figure 3.** Relationship between Gibbs free energy differences in solvent and gas environments ($\Delta\Delta G_{solvent-gas}$) and potential energy density differences in solvent and gas environments ($\Delta\Delta V_{solvent-gas}$), see text for an explanation of these terms.

increase of the relative stability of conformers when solvation takes place.

It can also be observed from Table 3 that bifurcated hydrogen bonds are present in almost all conformers. Conformers **3a**, **3b** (only when solvents effects are considered), **3c**, and **1a** exhibit bifurcated hydrogen bonds, in which an H atom is surrounded by three electronegative atoms, being covalently bonded to one of the electronegative atoms and hydrogen-bonded to the other two atoms.[8] Furthermore, conformer **2b** shows one oxygen atom forming two hydrogen bonds.

The preferred anomeric configuration of then β isomer of peracetylated *N*-D-mannosyl methanesulfonamide has been assigned by high-resolution NMR spectroscopy.[7] As sulfonamidoglycosylation afforded exclusively the β anomer, NMR studies of the α anomer could not be performed. Table 4 compares experimental and calculated $^1$H and $^{13}$C chemical shifts for the β anomer. Figure 4 shows the correlation between experimental and calculated values. In those cases in which a single signal due to several equivalent atoms is experimentally observed, the corresponding calculated chemical shifts of the involved atoms are averaged. It can be seen from the table that the agreement with experimental data is quite good in general. The largest error in $^1$H chemical shifts is observed for NH of the sulfonamide group and could be attributed to intermolecular hydrogen bonds formed in solution, which could not be mimicked by an implicit method like C-PCM.

Sulfonamidoglycosylation of peracetylated D-mannose with methanesulfonamide afforded the D-mannosyl methanesulfonamide with excellent β-stereoselectivity. The present results show the same anomeric ratio in the gas phase or when solvent effects (acetonitrile) are considered implicitly, which seems to indicate that the synthesis of the sulfonamide under study should occur mainly under thermodynamic control.

**Table 4**
Experimental and gas-phase calculated $^{1}H$ and $^{13}C$ chemical shifts, in ppm, of 2,3,4,6-tetra-*O*-acetyl-β-D-mannopyranosyl methanesulfonamide

| Atom | Experimental | Calculated |
|---|---|---|
| C1 | 80.60 | 82.94 |
| C2 | 69.77 | 73.64 |
| C3 | 71.53 | 74.01 |
| C4 | 65.51 | 67.40 |
| C5 | 74.02 | 77.75 |
| C6 | 62.63 | 65.76 |
| C7 | 170.33 | 168.81 |
| C8 | 21.04 | 21.78 |
| C9 | 169.90 | 168.39 |
| C10 | 20.94 | 21.60 |
| C11 | 170.04 | 168.56 |
| C12 | 20.69 | 21.47 |
| C13 | 170.68 | 169.00 |
| C14 | 20.89 | 21.58 |
| C15 | 43.53 | 49.41 |
| RMSD | | 0.67 |
| H1 | 5.03 | 5.19 |
| H2 | 5.43 | 5.53 |
| H3 | 5.10 | 5.46 |
| H4 | 5.10 | 5.46 |
| H5 | 3.73 | 3.92 |
| H6a,b | 4.17 | 4.16 |
| NH | 5.85 | 4.56 |
| H8a,b,c | 2.06 | 2.06 |
| H10a,b,c | 2.04 | 2.02 |
| H12a,b,c | 1.96 | 1.95 |
| H14a,b,c | 2.19 | 2.18 |
| H15a,b,c | 3.08 | 3.08 |
| RMSD | | 0.12 |

Calculated chemical shifts are presented as a Maxwell–Boltzmann statistical average of conformers **3**.

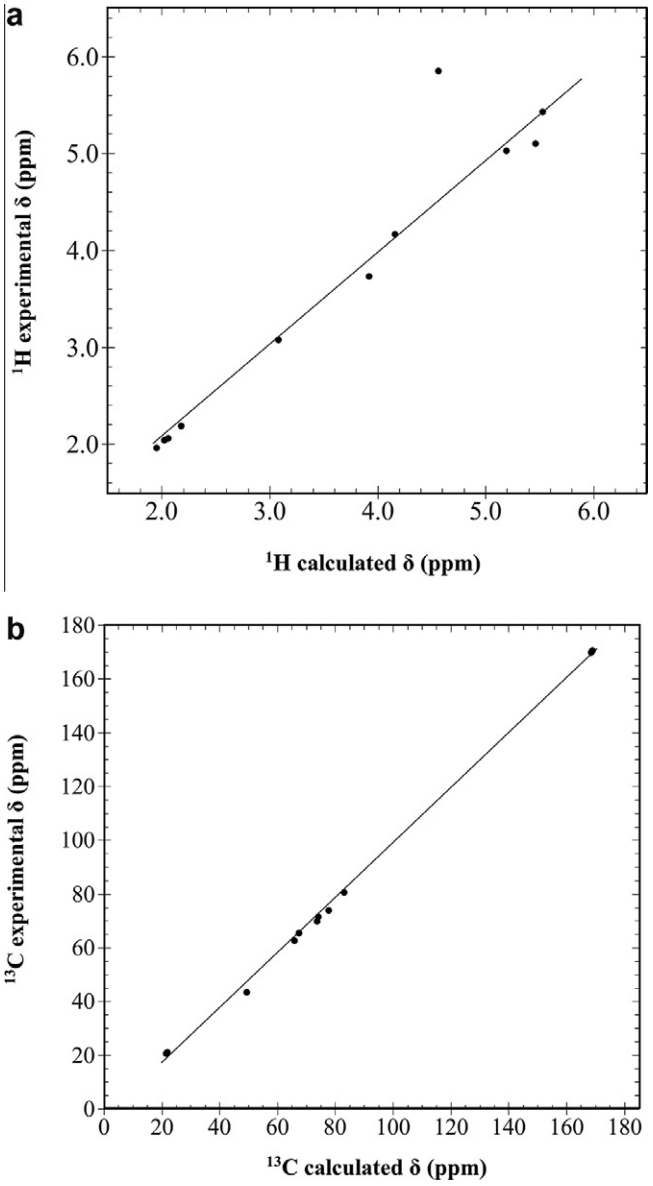



**Figure 4.** Comparison of calculated and experimental results of $^{13}C$ and $^{1}H$ NMR for 2,3,4,6-tetra-*O*-acetyl-β-D-mannopyranosyl methanesulfonamide. Theoretical chemical shifts were calculated in the gas phase.

Several *N*-glycosyl sulfonamides have been prepared by sulfonamidoglycosylations of carbohydrate derivatives (Scheme 1). The stereochemical outcome could be explained in terms of the conformational behavior of hex-2-enopyranosyl and pyranosyl sulfonamides.[4] In the present system the β anomer is favored by steric effects in the axial isomer accentuated by an $n_{N1} \rightarrow \sigma^{*}_{C1-O5}$ orbital interaction (*exo*-anomeric effect). An *anti* relationship between NH and anomeric hydrogen would permit an expression of the *exo*-anomeric interaction in the α anomer. This conformation necessarily points the hydrogen atom on nitrogen under the pyranose ring, giving an accentuated steric effect.[9] Close inspection to the dihedral angle between NH and the hydrogen of C1 in isomer **1a** shows a value of 102.4°, which is consistent with the presence of a *gauche* relationship between these hydrogens, but not an *anti* relationship. This conformation relieves the steric hindrance but not allows the expression of *exo*-anomeric effect, thus favoring the β isomer.[10]

On the other hand we have previously shown that in 2,3-enopyranosyl sulfonamides,[11] dihedral angles indicated an almost planar conformation of C1–C2–C3–C4, thus the unfavorable steric interaction described is absent in the α isomer, which enables the *exo*-anomeric interaction and a $n_{O5} \rightarrow \sigma^{*}_{C1-N1}$ orbital interaction (*endo*-anomeric effect) that are only present in the α isomer. Thus the stereochemical outcome of the sulfonamidoglycosylations would be controlled by the expression of $n_{N1} \rightarrow \sigma^{*}_{C1-O5}$ *exo*-anomeric and $n_{O5} \rightarrow \sigma^{*}_{C1-N1}$ *endo*-anomeric interactions, and steric effects.

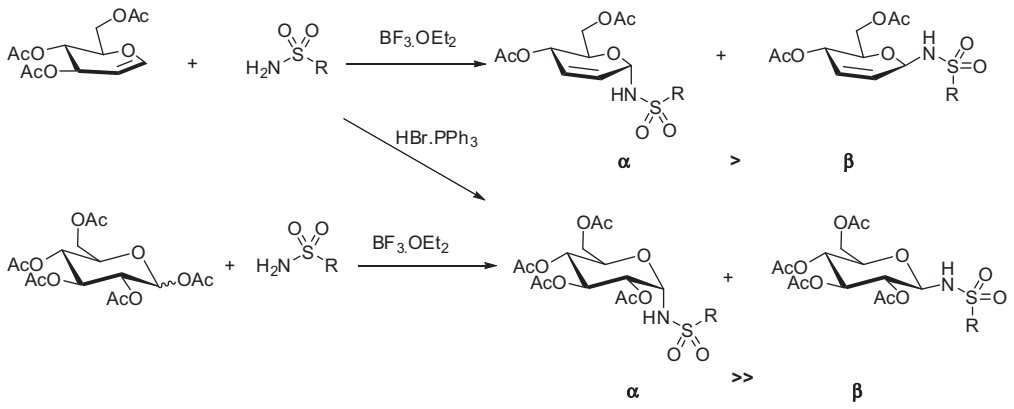
## 3. Conclusions

The conformational behavior of 2,3,4,6-tetra-*O*-acetyl-β-D-mannopyranosyl methanesulfonamide has been investigated from a combined theoretical and experimental point of view. The study of the conformational space of the above sulfonamide revealed that the β anomer is thermodynamically more stable than the α one. As the synthesis technique provides stereoselectivity to the β form, it is concluded that reaction takes place under thermodynamic control.

Several intramolecular hydrogen bonds were found in the stable conformers of the *N*-mannopyranosyl sulfonamide under study. A linear relationship was found to exist between the increase in the relative stability of the conformers and the strengthening of intramolecular hydrogen bonds after solvent effects are accounted for in the calculations.

A detailed analysis of geometrical parameters shed light into the nature of the solid state structure of the novel 2,34,6-tetra-*O*-acetyl-β-D-mannopyranosyl methanesulfonamide in terms of *exo*- and *endo*-anomeric effects and antiperiplanar relationships. NBO calculations confirmed those findings. Moreover, optimized geometries agree quite well with the crystallographic data.

Theoretical calculations of $^{13}C$ and $^{1}H$ NMR chemical shifts contribute to a better understanding of the experimental spectra.




**Scheme 1.**

Present results support previous findings concerning configuration and conformation assignments for 2,3,4,6-tetra-*O*-acetyl-β-D-mannopyranosyl methanesulfonamide. Furthermore, present results suggest that the NH group could be involved in intermolecular hydrogen bonds as experimental and theoretical chemical shifts exhibit appreciable discrepancies.

Finally, an explanation of the stereochemical outcome of sulfonamidoglycosylations, was given in terms of *exo*- and *endo*-anomeric effects and steric factors.

## 4. Experimental

### 4.1. General

NMR spectra were recorded at room temperature on a Varian Mercury 200 spectrometer. $^1$H NMR spectra were measured at 200 MHz and $^{13}$C spectra at 50 MHz in $CD_3CN$ solution, using the standard pulse sequence and procedures.

### 4.2. Preparation of 2,3,4,6-tetra-*O*-acetyl-β-D-mannopyranosyl methanesulfonamide

To a vigorously stirred solution of per-*O*-acetylated mannose (1 mmol) and methanesulfonamide (2 equiv) in MeCN (4 mL) under an Ar atmosphere, was added dropwise 2 equiv of $BF_3.Et_2O$. Once the reaction was completed (indicated by TLC, hexane/EtOAc 1:1), it was quenched by the addition of aq. $NaHCO_3$ (2 mL).

The reaction mixture was extracted with $CH_2Cl_2$ (3 × 5 mL) and the combined organic layers were washed with brine (2 × 5 mL), dried over $Na_2SO_4$, and evaporated. The residue was purified by crystallization from hexane–EtOAc.

### 4.3. X-ray diffraction data

Good-quality single crystals, suitable for X-ray analysis, were obtained upon crystallization from a solution of 2,3,4,6-tetra-*O*-acetyl-β-D-mannopyranosyl methanesulfonamide in EtOAc–hexane.

The measurements were performed on an Oxford Xcalibur Gemini, Eos CCD diffractometer with graphite-monochromated CuKα ($\lambda$ = 1.54178 Å) radiation. X-ray diffraction intensities were collected (ω scans with ϑ and κ-offsets), integrated and scaled with CrysAlisPro[12] suite of programs. The unit cell parameters were obtained by least-squares refinement (based on the angular settings for all collected reflections with intensities larger than seven times the standard deviation of measurement errors) using CrysAlisPro. Data were corrected empirically for absorption employing the multi-scan method implemented in CrysAlisPro. The structure was solved by direct methods with SHELXS-97[13] and the molecular model refined by full-matrix least-squares procedure on $F^2$ with SHELXL-97.[14] Hydrogen atoms were refined employing the riding model with the methyl group treated as a rigid group allowed to rotate around the corresponding C–C bond. Crystal data and structure refinement results are summarized in Table 5. Atomic coordinates, bond lengths and angles, and thermal parameters have been deposited by the Cambridge Crystallographic Data Centre (see below).

### 4.4. Computational method

The conformational space of the starting conformations (**1**–**4**) is investigated using genetic algorithm as implemented in Balloon[15] with default parameters. Those generated geometries are then optimized using the semiempirical PM6[16] method with MOPAC package.[17]

**Table 5**
Crystal data and structure refinement for 2,3,4,6-tetra-*O*-acetyl-β-D-mannopyranosyl methanesulfonamide

| | |
|---|---|
| Empirical formula | $C_{15}H_{23}NO_{11}S$ |
| Formula weight | 425.40 |
| Temperature | 293(2) K |
| Wavelength | 1.54184 Å |
| Crystal system | Orthorhombic |
| Space group | P $2_1$ $2_1$ $2_1$ |
| Unit cell dimensions | $a$ = 9.3970(9) Å |
| | $b$ = 10.4818(10) Å |
| | $c$ = 20.278(2) Å |
| Volume | 1997.3(3) Å 3 |
| $Z$ | 4 |
| Density (calculated) | 1.415 Mg/m3 |
| Absorption coefficient | 1.973 mm$^{-1}$ |
| $F$(000) | 896 |
| Crystal size | 0.105 × 0.242 × 0.302 mm |
| Theta range for data collection | 4.36–74.11° |
| Index ranges | $-7 \leqslant h \leqslant 11$, $-12 \leqslant k \leqslant 12$, $-25 \leqslant l \leqslant 25$ |
| Reflections collected | 6829 |
| Independent reflections | 3681 [$R$(int) = 0.0239] |
| Completeness to theta = 74.11° | 98.0 % |
| Absorption correction | Semi-empirical from equivalents |
| Max. and min. transmission | 1.00000 and 0.31295 |
| Refinement method | Full-matrix least-squares on F2 |
| Data/restraints/parameters | 3681/0/259 |
| Goodness-of-fit on F2 | 1.111 |
| Final R indices [I > 2sigma(I)] | R1 = 0.0493, wR2 = 0.1187 |
| $R$ indices (all data) | R1 = 0.0619, wR2 = 0.1304 |
| Absolute structure parameter | 0.00(3) |
| Extinction coefficient | 0.00030(17) |
| Largest diff. peak and hole | 0.355 and −0.239 e.Å$^{-3}$ |

The PM6-optimized geometries are further optimized using tools from the density functional theory[18–20] as implemented in the Gaussian 03 package.[21] The optimizations are accomplished using the Becke's three parameters hybrid density functional[22] with the gradient-corrected correlation functional due to Lee, Yang, and Parr,[23] a combination that gives rise to the well known B3LYP method.[24] Only those optimized geometries lying up to 3 kcal $mol^{-1}$ above the lowest-energy conformer of every molecule are considered for further studies. The energy threshold of 3 kcal $mol^{-1}$ provides some confidence that the contribution of higher energy conformations is less than 1% to every property measured at 298.15 K, according to the Maxwell–Boltzmann distribution. Basis sets are of double-zeta quality augmented with polarization and diffuse functions both in heavy and hydrogen atoms.

The Hessian matrix is calculated at the B3LYP/6-31++G(d,p) level of theory and it is diagonalized for all the optimized geometries to verify whether they are local minima or saddle points on the potential energy surface of the molecules.

To get an insight into the influence of the different anomeric effects over the relative stabilities of the conformers, a Natural Bond Orbital (NBO)[25] analysis is carried out at the B3LYP/6-31++G(d,p) level of theory. The Gaussian 03 package is used to this end.

The possibility of intramolecular hydrogen bonds in the glycosyl sulfonamide, as a potential fact in determining relative stabilities, is analyzed within the framework of the Atoms-in-Molecules (AIM) theory.[26] Electronic densities obtained at the B3LYP/6-31++G(d,p) level of theory and the AIMAll package[27] are used for the AIM study.

To analyze the effect of acetonitrile on the conformational behavior of the mannosyl sulfonamide, solvent effects are taken into account in the present calculations through the Conductor-like solvation model, as developed in the framework of the Polarizable Continuum Model (C-PCM).[28,29] Gas-phase geometries are re-optimized within the C-PCM model. Hessian matrices are constructed and diagonalized to confirm whether those structures are local minima or saddle points. Finally, the NBO and AIM analyses are performed on the freshly optimized geometries.

$^{1}H$ and $^{13}C$ isotropic shielding tensors are calculated at the B3LYP/6-31+G(d,p)[30] level of theory using the Gauge-Including Atomic Orbital method[31,32] as implemented in the Gaussian 03 package. C-PCM model with uaks radii is used to simulate acetonitrile effects. The isotropic shieldings are turned into chemical shifts by subtracting the corresponding isotropic shieldings of tetramethylsilane (TMS), which are calculated at the same level of theory.

A better comparison between experimental data and calculated properties could be obtained by including those conformers lying above the lowest-energy conformers up to 2 kcal $mol^{-1}$ in a Maxwell–Boltzmann statistical average at 298.15 K according to

$$\langle \delta \rangle = \frac{\sum_j \delta_j e^{-\frac{E_j}{RT}}}{\sum_j e^{-\frac{E_j}{RT}}}$$

where $\delta_j$ is the corresponding property, conformer contribution, and chemical shifts in the present work, of the jth conformer and $E_j$ is its relative energy.

## Acknowledgments

The authors thank CONICET (PIP 0137) and UNLP for the financial support. R.P.D., G.A.E., and P.A.C. are members of the Scientific Research Career of CONICET. M.J.L. is a fellow of CONICET

## Supplementary data

Supplementary data associated with this article can be found, in the online version, at http://dx.doi.org/10.1016/j.carres.2012.08.016.

## References

1. Ernst, B.; Magnani, J. L. *Nat. Rev. Drug Disc.* **2009**, *8*, 661–677.
2. Koester, D. C.; Holkenbrink, A.; Werz, D. B. *Synthesis* **2010**, 3217–3242.
3. Butera, A. P.; De Souza Filho, J. D.; Carvalho, D. T.; Figueiredo, R. C.; De Faria, L. C. A.; Nunes, M. A.; Prado, M. A. F.; Alves, R. J.; De Andrade, M. H. G.; Silva, K. T. S. *Quim. Nova* **2007**, *30*, 1267–1274.
4. Colinas, P. A. *Curr. Org. Chem.* **2012**, *16*, 1670–1679.
5. Crespo, R.; de Bravo, M. G.; Colinas, P. A.; Bravo, R. D. *Bioorg. Med. Chem. Lett.* **2010**, *20*, 6469–6471.
6. Rodríguez, O. M.; Maresca, A.; Témpera, C. A.; Bravo, R. D.; Colinas, P. A.; Supuran, C. T. *Bioorg. Med. Chem. Lett.* **2011**, *21*, 4447–4452.
7. Colinas, P. A.; Témpera, C. A.; Rodriguez, O. M.; Bravo, R. D. *Synthesis* **2009**, 4143–4148.
8. Rozas, I.; Alkorta, I.; Elguero, J. *J. Phys. Chem.* **1998**, *A102*, 9925–9932.
9. Pinto, B.; Schlegel, H.; Wolfe, S. *Can. J. Chem.* **1987**, *65*, 1658–1662.
10. A related explanation was used to analyze the conformational behavior of glycosylamines, see: Batchelor, R.; Green, D.; Johnston, B.; Patrick, B.; Pinto, B. *Carbohydr. Res.* **2001**, *330*, 421–426.
11. Lavecchia, M. J.; Diez, R. P.; Colinas, P. A. *Carbohydr. Res.* **2011**, *346*(3), 442–448.
12. CrysAlis CCD, CrysAlis RED and associated programs: Oxford diffraction (2006). Program name(s). Oxford diffraction Ltd, Abingdon, England.
13. Sheldrick, G. M. *Acta Crystallogr., Sect. A* **2008**, *64*, 112–122.
14. Johnson, C. K. *ORTEP-II. A Fortran Thermal-Ellipsoid Plot Program. Report ORNL-5318, Oak Ridge National Laboratory*; Tennessee: USA, 1976.
15. Vainio, M. J.; Johnson, M. S. *J. Chem. Inf. Model.* **2007**, *47*, 2462–2474.
16. Stewart, J. J. P. *J. Mol. Model.* **2007**, *13*, 1173–1213.
17. MOPAC2009: James, J. P.; Stewart. *Stewart Computational Chemistry*; Colorado Springs, CO.: USA, 2008 http://OpenMOPAC.net.
18. Hohenberg, P.; Kohn, W. *Phys. Rev.* **1964**, *136*, B864–B871.
19. Kohn, W.; Sham, L. *J. Phys. Rev.* **1965**, *140*, A1133–A1138.
20. Parr, R.; Yang, W. *Density Functional Theory of Atoms and Molecules*; Oxford University Press, 1989.
21. Frisch, M. J.; Trucks, G. W.; Schlegel, H. B.; Scuseria, G. E.; Robb, M. A.; Cheeseman, J. R.; Montgomery, J. A., Jr.; Vreven, T.; Kudin, K. N.; Burant, J. C.; Millam, J. M.; Iyengar, S. S.; Tomasi, J.; Barone, V.; Mennucci, B.; Cossi, M.; Scalmani, G.; Rega, N.; Petersson, G. A.; Nakatsuji, H.; Hada, M.; Ehara, M.; Toyota, K.; Fukuda, R.; Hasegawa, J.; Ishida, M.; Nakajima, T.; Honda, Y.; Kitao, O.; Nakai, H.; Klene, M.; Li, X.; Knox, J. E.; Hratchian, H. P.; Cross, J. B.; Bakken, V.; Adamo, C.; Jaramillo, J.; Gomperts, R.; Stratmann, R. E.; Yazyev, O.; Austin, A. J.; Cammi, R.; Pomelli, C.; Ochterski, J. W.; Ayala, P. Y.; Morokuma, K.; Voth, G. A.; Salvador, P.; Dannenberg, J. J.; Zakrzewski, V. G.; Dapprich, S.; Daniels, A. D.; Strain, M. C.; Farkas, O.; Malick, D. K.; Rabuck, A. D.; Raghavachari, K.; Foresman, J. B.; Ortiz, J. V.; Cui, Q.; Baboul, A. G.; Clifford, S.; Cioslowski, J.; Stefanov, B. B.; Liu, G.; Liashenko, A.; Piskorz, P.; Komaromi, I.; Martin, R. L.; Fox, D. J.; Keith, T.; Al-Laham, M. A.; Peng, C. Y.; Nanayakkara, A.; Challacombe, M.; Gill, P. M. W.; Johnson, B.; Chen, W.; Wong, M. W.; Gonzalez, C.; and Pople, J. A., Gaussian 03, revision d.01 [computer software] 2004.
22. Becke, A. *J. Chem. Phys.* **1993**, *98*, 5648–5652.
23. Lee, C.; Yang, W.; Parr, R. G. *Phys. Rev. B* **1988**, *37*, 785–789.
24. Stephens, P.; Devlin, F.; Chabalowski, C.; Frisch, M. *J. Phys. Chem.* **1994**, *98*, 11623–11627.
25. Reed, A. E.; Curtiss, L. A.; Weinhold, F. *Chem. Rev.* **1988**, *88*, 899–926.
26. Bader, R. *Atoms in Molecules. A Quantum Theory. International Series of Monographs on Chemistry*, Clarendon Press: Oxford, 1990.
27. Keith, T. A. Aimall version 09.02.01 [computer software], aim.tkgristmill.com, 2009.
28. Barone, V.; Cossi, M. *J. Phys. Chem. A* **1998**, *102*, 1995–2001.
29. Cossi, M.; Rega, N.; Scalmani, G.; Barone, V. *J. Comput. Chem.* **2003**, *24*, 669–681.
30. Cheeseman, J. R.; Trucks, G. W.; Keith, T. A.; Frisch, M. J. *J. Chem. Phys.* **1996**, *104*, 5497–5509.
31. Ditchfield, R. *Mol. Phys.* **1974**, *27*, 789–807.
32. Wolinski, K.; Hinton, J. F.; Pulay, P. *J. Am. Chem. Soc.* **1990**, *112*, 8251–8260.